doi.org/10.36721/PJPS.2024.37.4.REG.873-879.1

Imiquimod inhibits U87 cell proliferation and migration *in vitro* through inhibition of STAT-3/NF-κB signalling pathway

Shu Wang[1], Lu Yin[1], Hongbin Liu[1], Jiazhi Xu[1], Jibo Zhao[1], Yunzhi Pan[1] and Yurong Sun[2]*

[1]Department of Neurology, The Third Affiliated Hospital of Qiqihar Medical University, Tiefeng District, Qiqihar City, Heilongjiang Province, 27 Taishun Street, China

[2]School of Pathology, Qiqihar Medical University, Buqui North Street, Jianhua District, Qiqihar City, Heilongjiang Province, China

Abstract: Imiquimod, known for its immune-modulating properties, has emerged as a potential anti-cancer agent. The U87 glioblastoma cell line, known for its high malignancy and poor prognosis, presents a significant challenge in neuro-oncology. Targeting the STAT-3/NF-κB pathways offers a promising therapeutic strategy for glioblastoma treatment. Imiquimod potentially inhibits these oncogenic signaling routes to suppress U87 cell proliferation and migration. We investigated the effect of imiquimod (IMQ) on U87 cell growth using CCK-8 and cell scratch assays. Western blotting analyzed protein levels of STAT-3, p-STAT-3, NF-κB, and p-NF-κB, while flow cytometry assessed U87 cell apoptosis rates. ELISA detected cellular inflammatory factor levels. *In vivo* experiments further evaluated IMQ's impact on U87 cell growth. Findings suggest that IMQ suppresses U87 cell growth and movement, inhibits STAT-3 and NF-κB phosphorylation, and accelerates apoptosis. ELISA assays indicated that IMQ reduced local inflammation. Adding a STAT-3 inhibitor yielded similar effects to IMQ, altering cell proliferation, migration, and apoptosis. Overall, IMQ appears to inhibit U87 cell proliferation and migration, inducing programmed cell death through STAT-3 modulation.

Keywords: Imiquimod, glioma, U87 cells, cell proliferation, cell migration.

INTRODUCTION

Neurogliomas are the predominant primary cancerous growths in the central nervous system, characterized by frequent relapse and high fatality rates (Fan *et al*., 2023; Li *et al*., 2020). The tumors are classified into grades I to IV according to their malignancy, with the fastest growing, most malignant and incurable tumor subtype being glioblastoma. Still, gliomas remain one of the deadliest human cancers. Nonetheless, advancements have been achieved in diagnostic techniques and therapeutic approaches for gliomas, such as surgical removal combined with additional drug therapy or concurrent radiotherapy (Wu *et al*., 2018). The rate of survival after five years for patients with gliomas is still limited. The average median survival of patients with advanced glioblastoma remains less than 15 months, with only 3.3% of GBM patients surviving more than two years (Anton *et al*., 2012; Huang *et al*., 2017). Therefore, how to promote apoptosis and inhibit the value-added migration of glioblastoma has become the focus of researchers.

Imiquimod (IMQ) is a medication that activates toll-like receptor 7 (TLR7) and is employed in medical practice to treat surface-level basal cell carcinoma (BCC), in situ squamous cell carcinoma of the skin and metastatic cutaneous malignant melanoma (Garcia-Mouronte *et al*., 2023; Schon and Schön, 2006). The main mechanism of action of imiquimod (IMQ) is to activate specific receptors (TLR7) in the immune system, promote local immune responses, and increase the immune system's attack on tumor cells in the body (Joseph *et al*., 2024). IMQ also generates effects not dependent on TLR7 in various cancer cells, including sparking inflammasome activation through the ROS-dependent NLRP3 pathway, prompting cell death through the mitochondrial pathway, and initiating autophagy-mediated cell demise (Huang *et al*., 2010; Schon and Schon, 2007). Meanwhile, IMQ can T cell-mediated modulation of NF-κB, STAT-3, etc. In various types of skin cancer cells, leading to programmed cell death and cellular self-digestion (Nadeem *et al*., 2020). Here, we further demonstrate that IMQ regulates inflammatory factor secretion, apoptosis, value-addition and migration of U87 cells through NF-κB, STAT-3 axis.

MATERIALS AND METHODS

Cell culture

The U87 human glioma cell line was grown in a minimal essential medium enriched with 10% fetal bovine serum (FBS) sourced from Corning, New York, USA and 1% penicillin-streptomycin obtained from Gibson, Paisley, Scotland, UK. The cells were then placed in an incubator at 37 degrees Celsius with a gas mixture of 95% oxygen and 5% carbon dioxide.

Partition the U87 cells into four categories: A control cohort, an IMQ group treated with 1mmol/L concentration, a 5mmol/L IMQ-treated cohort, and a group subjected to 5mg/L IMQ in combination with compound 7d. The 1mmol/L IMQ group and 5mmol/L IMQ group received treatments with corresponding

**Corresponding author:* e-mail: 18043984765@163.com

concentrations of IMQ (Med Chem Express). U87 cells were treated with 1mmol/L and 5mmol/L IMQ (Med Chem Express), respectively and the 5mmol/L IMQ+ Compound 7 d group was treated with 10μmol/L Compound [STAT-3 inhibitor (STAT-3-IN), Med Chem Express] added to the 5 mmol/L IMQ group for 7 d. The Con group was a control group of U87 cells cultured in standard culture without stimulation. U87 cells served as the reference group.

Cell viability assay

Follow the manufacturer's guidelines to utilize the Cell Count Kit-8 (CCK-8) assay from Sigma, USA, for assessing cell proliferation. Cells were treated with 1mmol/L IMQ, 5mmol/L IMQ, 5mmol/L IMQ and STAT-3 inhibitor (Compound 7d) for 24h. Then, CCK-8 was added to the wells and examined 1h later. Measure absorbance at 450nm.

Elisa

Measure the concentrations of TNF-α and IL-6 in U87 cells across all experimental groups. The U87 cells were individually grown in 6-well culture dishes. Subsequent to various interventions, the culture solution was harvested and subjected to centrifugation at 8000 rotations per minute for 30 minutes at 4 degrees Celsius. Follow the guidelines provided by the manufacturer (Sigma, USA) to utilize an ELISA kit for quantifying the levels of soluble/insoluble TNF-α and IL-6. Utilize a tablet reader specifically designed for enzyme assays to read the absorbance at 450nm.

Wound Healing Analysis

As mentioned in Cory's investigation on scratch wound assessment, experiments on wound healing were conducted to assess the migratory capability of cells. The protocol and statistical analysis for wound healing determination were carried out following the techniques described in Chen *et al*. research on how tetrachlorodibenzo-p-dioxin enhances the migratory ability of primary rat astrocytes cultured through the aromatic hydrocarbon receptor pathway. In brief, prior to cell seeding, use a marker pen to create three parallel marks at the base of each well in a sterile 6-well plate to indicate the wound area for imaging. Subsequently, cells in the logarithmic growth phase were seeded onto the culture plate at a concentration of 2 × 105 cells/ml and cultured until a confluence level exceeding 95% was attained. Subsequently, the cell monolayer was scratched using the tip of a 1 mL pipette to create a wound. Several crosses were marked within the wound and the parallel lines using the marker pen and the regions spanning the lines within the wound were designated as the positions for capturing images. Any detached cells were washed away with phosphate buffer and the cells were then cultured in a low-serum (1% FBS) medium supplemented with various compounds. Photographs of the specified wound regions were taken at 0-24 hours post-treatment using an inverted microscope equipped with a digital camera.

At every time point, six pictures were taken and assessed for each well. Employ the Image Pro Plus 6 software developed by Media Cybernetics Inc. (USA) to assess cell movement and calculate the migration distance by dividing the decreased wound area in each picture by the initial wound length.

Trans well assay

The matrix (BD, USA) was defrosted overnight at 4 degrees Celsius. Afterwards, 100 micro liters of diluted matrix gel is administered into the laboratory apparatus. Subsequently, 200 micro liters of serum-free medium was introduced into the upper chamber and 500 micro liters of MEM supplemented with 10% FBS is added to the lower chamber. 2×105 harvested cells were seeded into the upper chambers and cultured in the incubator for an additional 24 hours. Following that, removed the invasive chamber, preserved the cells on the polycarbonate membrane using 4% para formaldehyde and dye them with 0.1% crystal violet. Chosen three random areas and enumerate the invading cells using a microscope. The trial was repeated three times.

Cell apoptosis assay by flow cytometry

Follow the instructions provided by the manufacturer to assess apoptotic cells using an apoptosis detection kit (Sigma, USA). Cells in the logarithmic growth phase were harvested and 500μl of binding buffer was used to suspend them. Equal volumes of 5μl Annexin V-APC and 5μl propidium iodide were added to the cells, which were then incubated for 10 minutes at room temperature in the absence of light. Flow cytometry was utilized to analyze the cells.

Western blot assay

Retrieved cellular proteins and quantify their concentration utilizing the Pierce BCA protein assay kit. Post-separation via 10% SDS-PAGE gel, transferred the segregated protein onto a polyvinylidene fluoride (PVDF) membrane. Next, obstruct the membrane in Tris-buffered saline Tween supplemented with 5% skim milk at ambient temperature for 60 minutes. Conduct protein blot analysis adhering to the standardized protocol. The primary antibodies utilized comprise STAT-3 (at a dilution of 1:1000, Abcam, England) and p-STAT-3 (concentrated at 1:1000, Abcam, England). Employed corresponding secondary antibodies including anti-mouse and anti-rabbit (both diluted at 1: 5000, Proteintech, China). X-ray film development is executed under subdued lighting conditions. Subsequently, proteins were distinguished utilizing enhanced chemiluminescence (ECL) with an exposure duration of approximately 60 seconds for scanning and quantification.

Tumor formation experiment in nude mice
Administered a U-373MG cell suspension, comprising 1x10^6 cells per milliliter, into the right axillary region of BALB/c nude mice to initiate a tumor model. When the tumor grew to about 100 mm3, the tumor-bearing nude mice were divided into control group and imiquimod group, with 10 in each group. The imiquimod group was given 0.5mM /d gavage of imiquimod. The control group was given normal saline for 20 days.

After administration, the nude mice were killed and the tumor volume and mass were detected. The tumor suppression rate was calculated, and the tumor suppression rate = (tumor mass of control group - tumor mass of experimental group)/tumor mass of control group ×100%. All experimental animal procedures were approved by the Ethics Committee of the Beijing Longan Laboratory Animal Breeding Centre (No. bjoronan-L-L-0713).

STATISTICAL ANALYSIS

Conduct statistical analysis utilizing GraphPad Prism 8.0 software. Present the data as mean value plus or minus standard deviation (x ± s). Group comparisons were conducted using one-way ANOVA, while the SNK-q test was employed for pairwise comparisons between groups.

RESULTS

IMQ regulates U87 cell proliferation
Cell proliferation assays were performed on the U87 cell line. Measurements by CCK-8 showed that IMQ inhibited the proliferation of U87 cells 24 hours after treatment and was positively correlated with IMQ concentration (fig.1 F). Additionally, we investigated whether STAT-3 played a role in the impact of IMQ on U87 cell migration and invasion. Specifically, comparative experiments were performed by adding or not adding STAT-3 inhibitors. We found that the addition of STAT-3 further inhibited the value-added of U87 (fig.1 A-E). In summary, IMQ may regulate U87 cell value-addition by modulating STAT-3.

IMQ regulates TNF-α and IL-6 expression levels
We further monitored the levels of inflammatory factors TNF-α and IL-6 expression in the cells of each group. ELISA results showed that TNF-α and IL-6 were significantly decreased in U87 cells treated with IMQ and STAT-3 inhibitors and the difference between groups was statistically significant ($p<0.05$)(fig. 2). This suggests that IMQ may regulate the cellular value-added and apoptotic situation by modulating inflammatory factors.

IMQ regulates migration and invasion of U87 cells
Afterwards, we performed trans well and scratch assays to assess the impact of IMQ on the migratory and invasive capacities of U87 cells. Both assays revealed a substantial reduction in the migration and invasion capabilities of U87 cells upon exposure to IMQ, with a positive correlation observed between the extent of inhibition and the concentration of IMQ. In addition, we investigated if STAT-3 played a role in mediating the impact of IMQ on the migratory and invasive properties of U87 cells. Specifically, comparative experiments were performed by adding or not adding STAT-3 inhibitors.

The addition of STAT-3 inhibitors led to a significant decrease in glioma cell migration and invasion (fig. 3).In comparison, the combination of IMQ and a STAT-3 inhibitor significantly reduced the migration and invasion of glioma cells more than IMQ alone. Our data suggest that IMQ may regulate the migration and invasion of glioma cells by targeting STAT-3.

IMQ-induced apoptosis of U87 cells
The exposure of phosphatidylserine on the outer membrane, a characteristic feature of apoptotic cells, has also been detected in other forms of programmed cell death. To investigate if similar mechanisms were triggered by IMQ treatment, U87 cells were exposed to 1 mmol/L IMQ, 5 mmol/L IMQ and 5 mmol/L IMQ+ Compound 7 d for 24 hours. Following exposure to 1mmol/L IMQ, 5mmol/L IMQ, and 5mmol/L IMQ+ compounds for 24 hours, U87 glioblastoma cells exhibited a notable and distinct rise in the quantity of annexin V/PI positive cells in comparison to the control group, with statistical significance ($p<0.05$)(fig. 4).

IMQ regulates STAT-3 and NF-κB protein expression levels.
The expression levels of STAT-3 and NF-κB proteins in each cell group were assessed via Western blotting. Relative to the control group, the protein levels of STAT-3, p-STAT-3, NF-κB and p-NF-κB in cells treated with 1mmol/L and 5mmol/L IMQ exhibited a notable reduction ($p<0.01$)(fig. 5).

The expression levels of the mentioned proteins were found to be directly associated with the concentration of IMQ. When comparing the 5mmol/L IMQ group with the 5mmol/L IMQ + compound 7d group, we observed a significant decrease in the expression levels of these proteins in the 5mmol/L IMQ + compound 7d group compared to the 5mmol/L IMQ group ($p<0.01$). This suggests that IMQ inhibits U87 cells by suppressing both the protein expression and phosphorylation of STAT-3, leading to inhibition of proliferation and migration while promoting apoptosis in U87 cells.

Effects of imiquimod on tumor growth in nude mice
Compared with the control group, the tumor mass and tumor volume in the imiquimod group were significantly reduced ($P<0.05$) as shown in fig. 6.

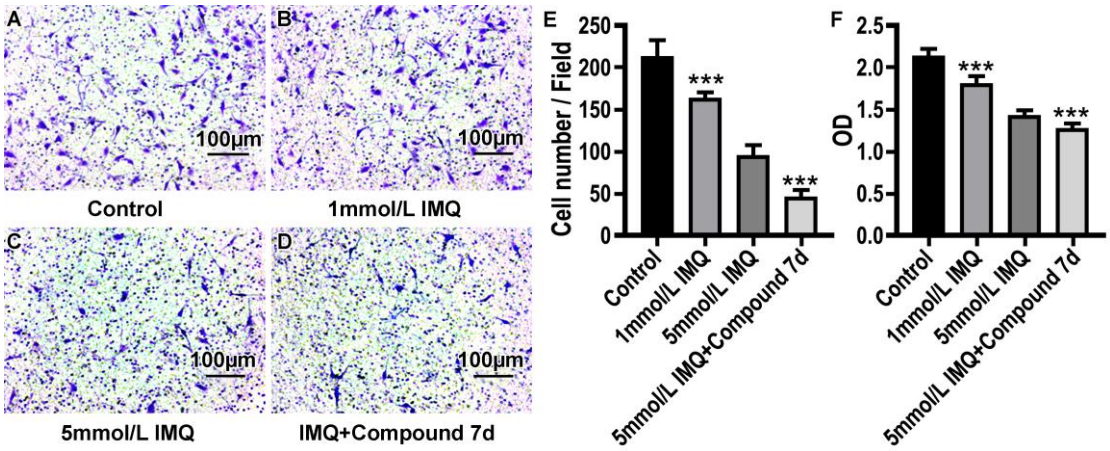

Fig. 1: Effect of IMQ on migration and invasion of U87 glioma cells. A-D, Representative images of migrated cells in each group. ×100 magnification. E, The effect of IMQ on U87 cell migration was analysed using Trans well migration assay. F, The effect of IMQ on the proliferation of U87 cells was assessed using CCK-8 assay.

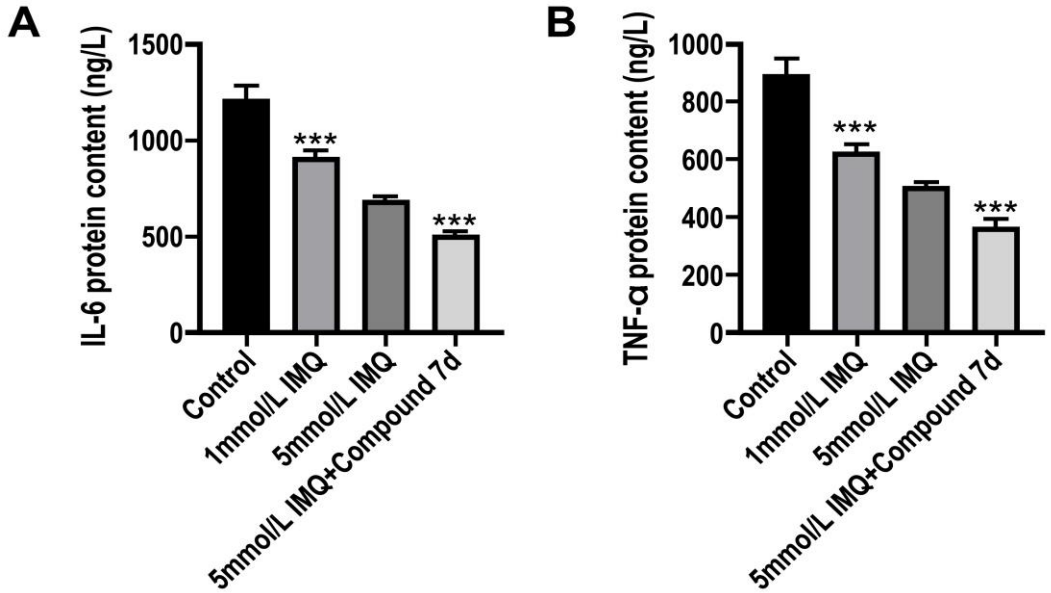

Fig. 2: IMQ can have regulate the secretion of inflammatory factors in U87 cells. A. IL-6 protein level. B. TNF-α protein level. Values are expressed as mean ±SD.

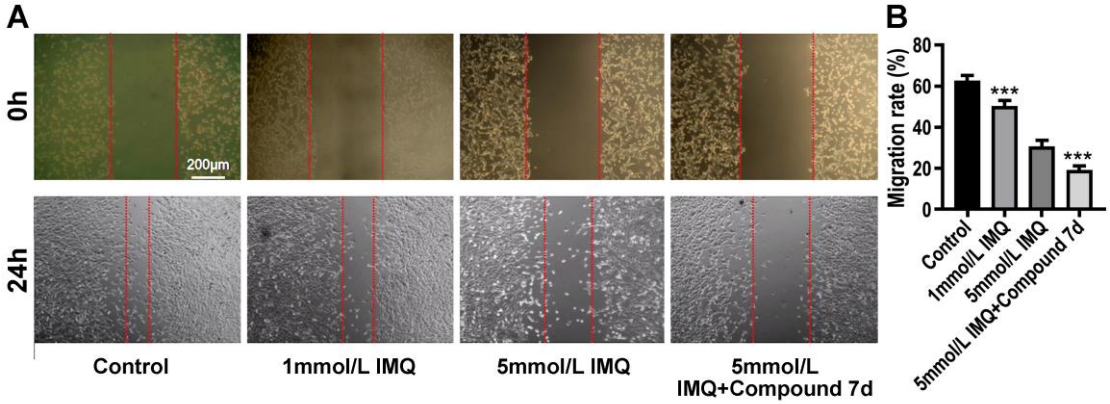

Fig. 3: Effect of IMQ on the proliferation of U87 glioma cells *in vitro*. A, Representative light microscopy images showing the migration of IMQ cells with different treatments towards the scratched area of cell stripping within 24 h. B, The corresponding cell migration rates are summarised.

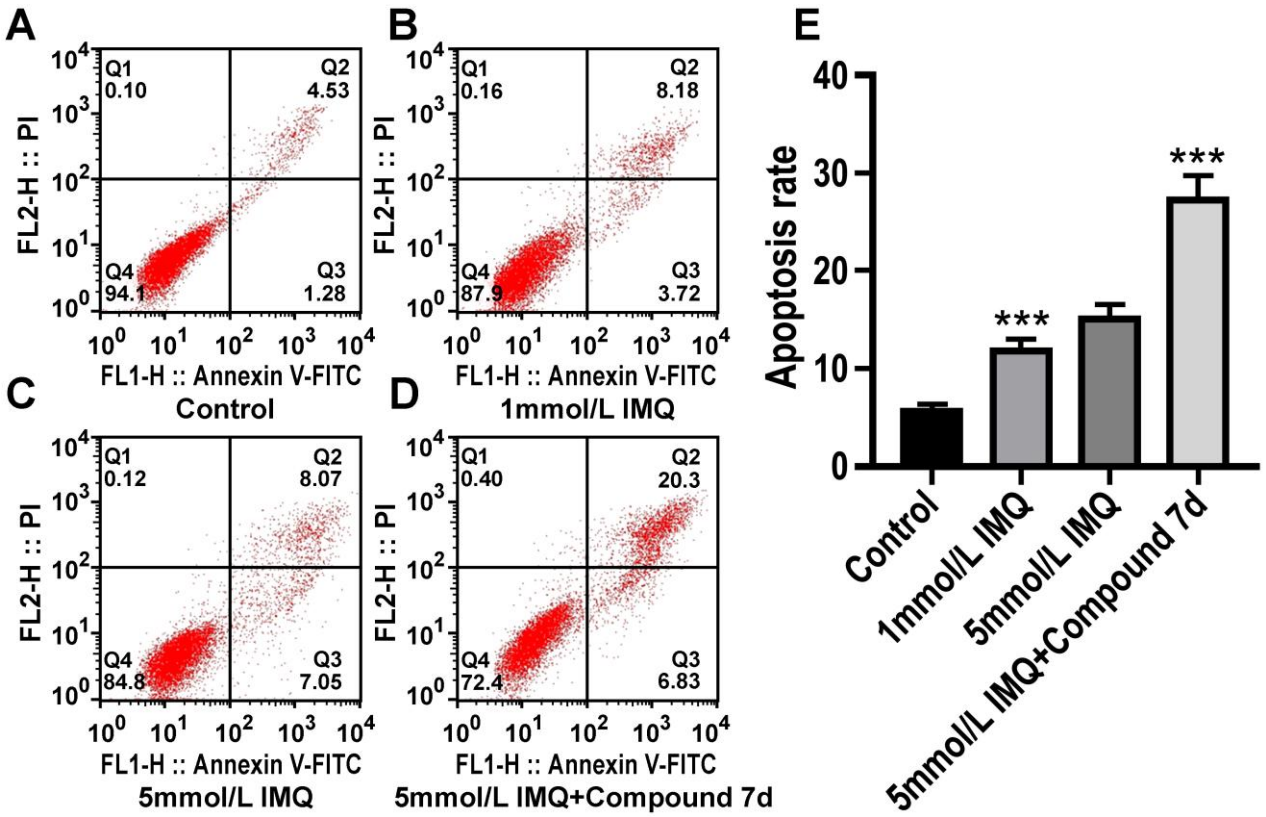

Fig. 4: Effect of IMQ on apoptosis of U87 glioma cells. a. Flow cytometry detection of the effect of IMQ on apoptosis in U87 glioma cells. B. The corresponding apoptosis rates are summarised.

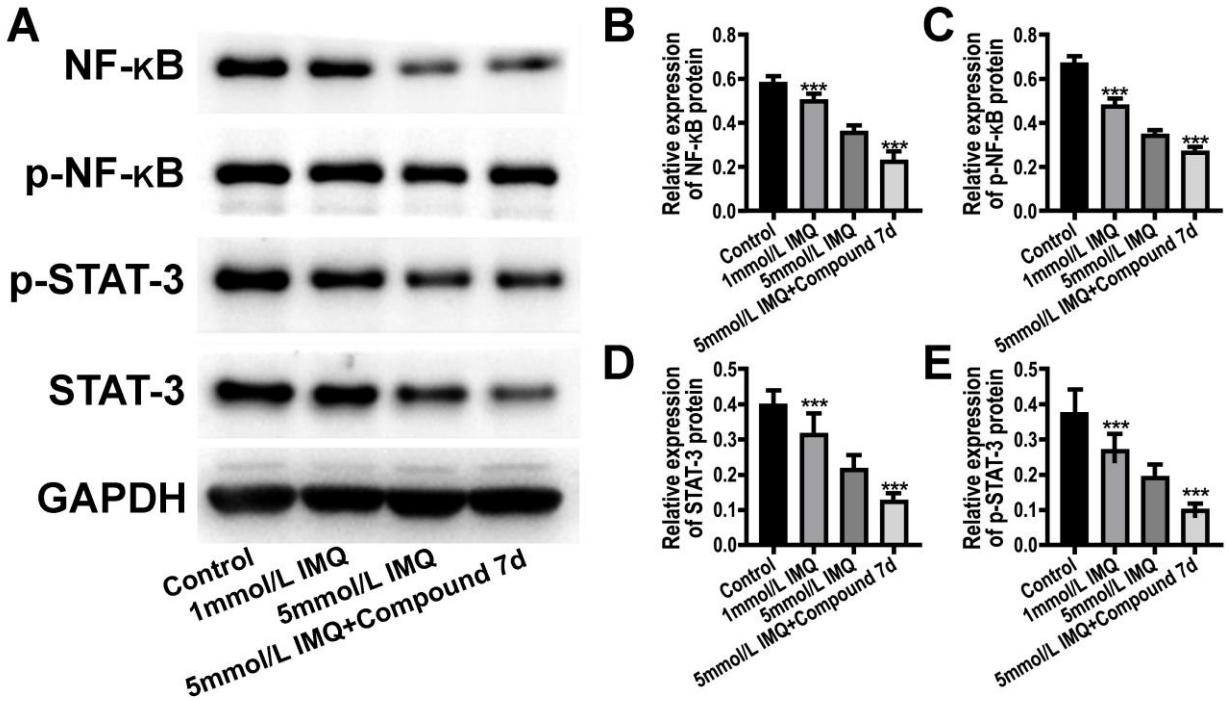

Fig. 5: Protein blot analysis revealed the presence of NF-κB in U87 MG cells, along with the expression levels of p-NF-κB, STAT-3 and p-STAT-3 proteins. (A) Expression levels of related proteins in different treatment groups. (B) Expression levels of NF-κB proteins in different groups. (C) Expression levels of p-NF-κB protein in different groups. (D) Expression levels of STAT-3 protein in different groups. (E) Expression levels of p-STAT-3 protein in different groups.

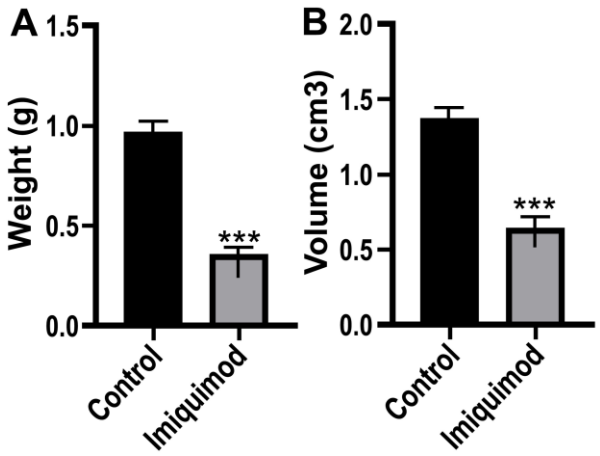

Fig. 6: The tumor volume and tumor were compared between the two groups. A, The tumor mass in the miquimod group showed a notable decrease compared to the control group. B, The volume of tumors in the miquimod-treated group exhibited a significant reduction in comparison to that of the control group.

DISCUSSION

Apoptosis is a well-preserved intrinsic process in eukaryotic cells that regulates programmed cell death. This process removes undesired or faulty cells through a systematic series of cellular breakdown steps without triggering inflammation (Divac Rankov *et al*., 2017; El-Khattouti *et al*., 2013). Beyond issues of unregulated cell division, substantial evidence indicates that proliferating tumors need anti-apoptotic mutations to ensure their survival and further proliferation (Ye *et al*., 2017). Restoring programmed cell death in cancerous cells by blocking survival mechanisms represents a hopeful strategy for cancer treatment.

Imiquimod acts as a TLR activator, triggering both innate and adaptive immune responses by binding to TLR7. This results in the activation of NF-κB and STAT-3, which promote the expression of inflammatory genes in plasmacytoid dendritic cells, such as TNF-α, interferon-a, and IL-12 (Trager *et al*., 2021). Beyond its impact on the NF-κB and STAT-3 signaling pathways, imiquimod also induces apoptosis (Li *et al*., 2023; Wu *et al*., 2020; Yang *et al*., 2019).

The antitumor effect of imiquimod has been demonstrated in various benign and malignant skin lesions (Yuan *et al*., 2018). Available clinical evidence suggests that IMQ has been used with some clinical success. For example, cervical squamous epitheliopathy, skin cancer and psoriasis (Fonseca *et al*., 2021; Garcia-Mouronte *et al*., 2023). This study proves that imiquimod directly reduces viability and induces apoptosis in the U87 cell line. We found that imiquimod not only reduces the occurrence of STAT-3 phosphorylation but also reduces the occurrence of NF-κB phosphorylation. Simultaneously, we found that IMQ exhibited cytotoxic effects, decreasing the survival of U87 MG cells and elevating the apoptosis rate to a certain degree, aligning with findings from prior research (Igari *et al*., 2019; Saikh and Ranji, 2021). According to previous studies, IMQ-induced cell injury and death involved multiple mechanisms, such as increased apoptosis, reactive oxygen species (ROS) production, mitochondrial damage, the role of AMPK and inhibition of STAT-3 and NF-κB pathways (Chuang *et al*., 2020; Srikanth and Rasool, 2022). Subsequently, we adopted the strategy of co-incubating IMQ with U87 cells. We observed that the migration and proliferation rates of U87 cells with the addition of IMQ appeared significantly reduced, indicating that the tumor proliferation and migration of U87 MG cells were inhibited. In animal studies, we found that the imiquimod group significantly inhibited tumor growth. Therefore, we believe that imiquimod is a drug that can effectively inhibit the proliferation of U87 cells (Wang *et al*., 2015; Yang *et al*., 2019). It could also be a new treatment for brain glioma.

CONCLUSION

In conclusion, we have clarified the molecular pathways responsible for imiquimod-triggered cell death in melanoma cells. Additionally, we have proposed a conceptual framework detailing the communication routes and crucial components crucial for controlling imiquimod-induced cell death in glioma cells. Miquimod has significant potential as a new method for cancer treatment. It enhances the immune response of the body to tumors through immune regulatory mechanisms, making it an important application prospect in cancer treatment. In vivo studies have laid the foundation for the clinical application of imiquimod and future research will continue to explore its efficacy, optimal application regimen and combination strategies with other treatment methods in various cancers. Therefore, our results indicate that using imiquimod in conjunction with STAT-3 blockers could be a promising advancement in glioma therapy.

ACKNOWLEDGEMENT

This study was supported by the Clinical Research Fund of Qiqihar Academy of Medical Sciences (QMSI2019L-29).

REFERENCES

Anton K, Baehring JM and Mayer T (2012). Glioblastoma multiforme: Overview of current treatment and future perspectives. *Hematol. Oncol. Clin. North Am.,* **26**(4): 825-853.

Chuang KC, Chang CR, Chang SH, Huang SW, Chuang SM, Li ZY, Wang ST, Kao JK, Chen YJ and Shieh JJ (2020). Imiquimod-induced ROS production disrupts the balance of mitochondrial dynamics and increases

mitophagy in skin cancer cells. *J. Dermatol Sci.,* **98**(3): 152-162.

Divac Rankov A, Ljujic M, Petric M, Radojkovic D, Pesic M and Dinic J (2017). Targeting autophagy to modulate cell survival: A comparative analysis in cancer, normal and embryonic cells. *Histochem Cell Biol.,* **148**(5): 529-544.

El-Khattouti A, Selimovic D, Haikel Y and Hassan M (2013). Crosstalk between apoptosis and autophagy: molecular mechanisms and therapeutic strategies in cancer. *J. Cell Death,* **6**: 37-55.

Fan K, Wei Y, Ou Y and Gong J (2023). Integrated analysis of multiple methods reveals characteristics of the immune microenvironment in medulloblastoma. *Brain Tumor Pathol.,* **40**(4): 191-203.

Fonseca BO, Possati-Resende JC, Salcedo MP, Schmeler KM, Accorsi GS, Fregnani J, Antoniazzi M, Pantano NP, Santana IVV, Matsushita GM and Dos Reis R (2021). Topical imiquimod for the treatment of high-grade squamous intraepithelial lesions of the cervix: A Randomized controlled trial. *Obstet. Gynecol.,* **137**(6): 1043-1053.

Garcia-Mouronte E, Berna-Rico E, de Nicolas-Ruanes B, Azcarraga-Llobet C, Alonso-Martinez de Salinas L and Bea-Ardebol S (2023). Imiquimod as local immunotherapy in the management of premalignant cutaneous conditions and skin cancer. *Int. J. Mol. Sci.,* **24**(13): 10835.

Huang J, Samson P, Perkins SM, Ansstas G, Chheda MG, DeWees TA, Tsien CI, Robinson CG and Campian JL (2017). Impact of concurrent chemotherapy with radiation therapy for elderly patients with newly diagnosed glioblastoma: A review of the National Cancer Data Base. *J. Neurooncol.,* **131**(3): 593-601.

Huang SW, Liu KT, Chang CC, Chen YJ, Wu CY, Tsai JJ, Lu WC, Wang YT, Liu CM and Shieh JJ (2010). Imiquimod simultaneously induces autophagy and apoptosis in human basal cell carcinoma cells. *Br. J. Dermatol.,* **163**(2): 310-320.

Igari S, Ohtsuka M and Yamamoto T (2019). Imiquimod-induced widespread psoriasiform eruptions. *Eur. J. Dermatol.,* **29**(2): 225-227.

Joseph T, Genkin M, Genkin A, Joseph J, Manuchian E and Ray K (2024). The efficacy of imiquimod-induced psoriasis model on murine cells. *Cureus.,* **16**(6): e62914.

Li C, Zou H, Xiong Z, Xiong Y, Miyagishima DF, Wanggou S and Li X (2020). Construction and validation of a 13-gene signature for prognosis prediction in medulloblastoma. *Front Genet.,* **11**: 429.

Li Y, Cui H, Li S, Li X, Guo H, Nandakumar KS and Li Z (2023). Kaempferol modulates IFN-γ induced JAK-STAT signaling pathway and ameliorates imiquimod-induced psoriasis-like skin lesions. *Int. Immunopharmacol.,* **114**: 109585.

Nadeem A, Ahmad SF, Al-Harbi NO, Ibrahim KE, Alqahtani F, As Sobeai HM and Alotaibi MR (2020). Inhibition of interleukin-2-inducible T-cell kinase causes reduction in imiquimod-induced psoriasiform inflammation through reduction of Th17 cells and enhancement of Treg cells in mice. *Biochimie.,* **179**: 146-156.

Saikh KU and Ranji CM (2021). Cells stimulated with more than one toll-like receptor-ligand in the presence of a myd88 inhibitor augmented interferon-β via myd88-independent signaling pathway. *Viral Immunol.,* **34**(9): 646-652.

Schon M and Schon MP (2007). The antitumoral mode of action of imiquimod and other imidazoquinolines. *Curr. Med. Chem.,* **14**(6): 681-687.

Schon MP and Schon M (2006). The small-molecule immune response modifier imiquimod--its mode of action and clinical use in the treatment of skin cancer. *Expert Opin. Ther. Targets.,* **10**(1): 69-76.

Srikanth M and Rasool M (2022). 3, 3'- diindolylmethane hinders IL-17A/IL-17RA interaction and mitigates imiquimod-induced psoriasiform in mice. *Int Immunopharmacol.,* **109**: 108795.

Trager MH, Rizk E, Rose S, Zhu K, Lau B, Fullerton BT, Pradhan J, Moore M, Srivastava AC, Singer G, Gartrell R, Chang R, Geskin LJ, Saenger YM and Goldenberg G (2021). Transcriptomic analysis identifies differences in gene expression in actinic keratoses after treatment with imiquimod and between responders and non responders. *Sci. Rep.,* **11**(1): 8775.

Wang ST, Huang SW, Kao JK, Liang SM, Chen YJ, Chen YY, Wu CY and Shieh JJ (2015). Imiquimod-induced AMPK activation causes translation attenuation and apoptosis but not autophagy. *J. Dermatol. Sci.,* **78**(2): 108-116.

Wu F, Zhao Z, Chai R, Liu Y, Wang K, Wang Z, Li G, Huang R, Jiang H and Zhang K (2018). Expression profile analysis of antisense long non-coding RNA identifies WDFY3-AS2 as a prognostic biomarker in diffuse glioma. *Cancer Cell Int.,* **18**: 107.

Wu S, Zhao M, Sun Y, Xie M, Le K, Xu M and Huang C (2020). The potential of diosgenin in treating psoriasis: Studies from HaCaT keratinocytes and imiquimod-induced murine model. *Life Sci.,* **241**: 117115.

Yang BY, Cheng YG, Liu Y, Liu Y, Tan JY, Guan W, Guo S and Kuang HX (2019). *Datura metel* L. ameliorates imiquimod-induced psoriasis-like dermatitis and inhibits inflammatory cytokines production through TLR7/8-MyD88-NF-κB-NLRP3 inflammasome pathway. *Molecules,* **24**(11): 2157.

Ye K, Wei Q, Gong Z, Huang Y, Liu H, Li Y and Peng X (2017). Effect of norcantharidin on the proliferation, apoptosis and cell cycle of human mesangial cells. *Ren Fail.,* **39**(1): 458-464.

Yuan J, Ni G, Wang T, Mounsey K, Cavezza S, Pan X and Liu X (2018). Genital warts treatment: Beyond imiquimod. *Hum. Vaccin. Immunother.,* **14**(7): 1815-1819.